

Effect of Single Heater Test on intact rock properties at Yucca Mountain, Nevada

N.S. Brodsky & G.T. Barker

Sandia National Laboratories, Albuquerque, New Mexico, USA

Sandia is a multiprogram laboratory operated by Sandia Corporation, a Lockheed Martin Company, for the United States Department of Energy under Contract DE-AC04-94AL85000.

RECEIVED
AUG 28 2000
OSTI

ABSTRACT: As part of ongoing investigations into locating a repository at Yucca Mountain Nevada, two in situ heated tests have been fielded underground at the Exploratory Studies Facility. The first of these tests utilized a single heater to elevate the temperature of a 13 m wide, 5.5. m tall, 8.5 m deep block that was exposed on three sides and attached on one side, on the top, and on the bottom. The objective of the work described here was to assess changes in thermal and mechanical properties of intact rock occurring as a result of conducting this in situ test.

1 INTRODUCTION

The Single Heater Test is fully described in Finley et al. (1998). Before the Single Heater Test (SHT) was initialized, pre-test characterization of the SHT block was conducted. One component of the pre-test characterization comprised thermal expansion, thermal conductivity, and unconfined compression tests, performed on intact core removed from instrumentation boreholes. These data are reported in Brodsky (1996) and Boyd et al. (1996) for thermal and mechanical properties, respectively. After the SHT block cooled, additional boreholes were drilled into the block, providing samples for laboratory testing of thermal and mechanical properties. Figure 1 shows a plan view of the SHT block, the post-test characterization drillholes (overcore holes 194 and 196; observation holes 199, 200, 202, and 203), and the location of the approximate maximum extent of the 100°C isotherm, with the long axis of the ellipse oriented along the axis of the heater.

The laboratory data are used to compare pre-test and post-test properties and also to examine post-test differences between rocks that were inside and outside of the approximate maximum extent of the 100°C isotherm. Pre-test thermal properties characterization tests were performed by Holometrix, Inc., and the pre-test mechanical tests were performed by New England Research. Additional Alcove 5 characterization data that will be used for comparisons were obtained in preparation for the Drift Scale Test (Brodsky 1997b) and for general Alcove 5 characterization (Brodsky 1997c).

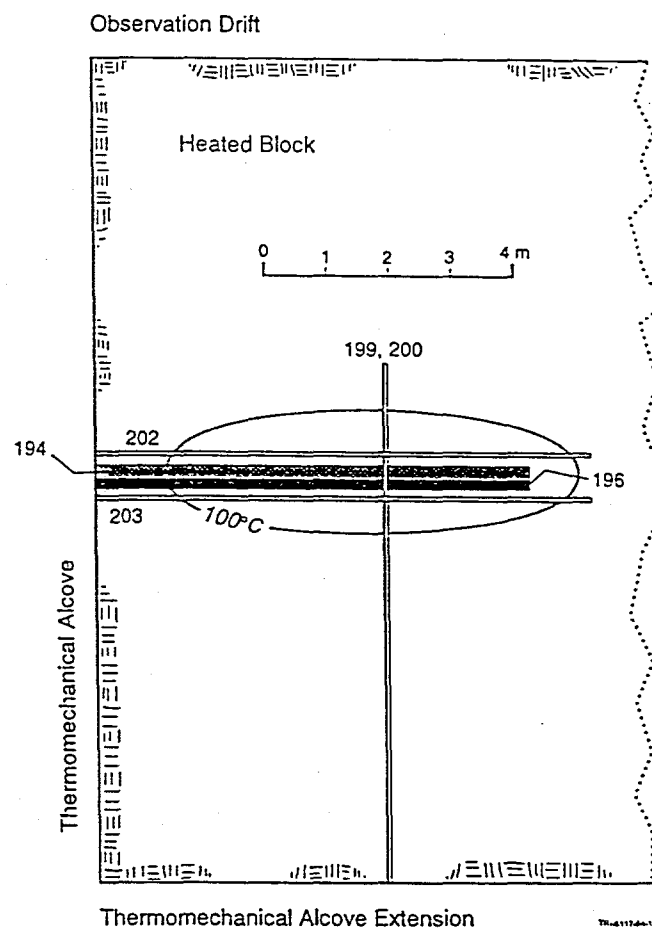


Figure 1. Plan view of SHT block showing locations of post-test overcores and boreholes.

DISCLAIMER

This report was prepared as an account of work sponsored by an agency of the United States Government. Neither the United States Government nor any agency thereof, nor any of their employees, make any warranty, express or implied, or assumes any legal liability or responsibility for the accuracy, completeness, or usefulness of any information, apparatus, product, or process disclosed, or represents that its use would not infringe privately owned rights. Reference herein to any specific commercial product, process, or service by trade name, trademark, manufacturer, or otherwise does not necessarily constitute or imply its endorsement, recommendation, or favoring by the United States Government or any agency thereof. The views and opinions of authors expressed herein do not necessarily state or reflect those of the United States Government or any agency thereof.

DISCLAIMER

**Portions of this document may be illegible
in electronic image products. Images are
produced from the best available original
document.**

2 SAMPLE ACQUISITION AND SPECIMEN PREPARATION

All specimens are from the Tptpmn (Topopah Spring tuff, crystal poor, middle nonlithophysal) lithostratigraphic unit and from the TSw2 (Topopah Spring welded unit 2) thermal/mechanical (T/M) unit. The borehole designation as well as the distance (in feet) from the borehole collar are incorporated into the specimen identification number. The thermal expansion specimens are the same dimensions as the pre-test characterization specimens. The pre-test thermal conductivity specimens were 50.8 mm in diameter whereas these post-test specimens are 38.1 mm. The pre-test characterization mechanical test specimens were 41.9 mm in diameter and 101.6 mm in length. The pre-test specimens are very close in dimension and in length-to-diameter ratio to the post-test specimens used in this study.

All specimens (with the exception of two saturated pre-test mechanical characterization specimens) were tested in the air-dried state (i.e. no effort was made to preserve or alter the moisture content). The moisture content during testing was substantially different from in situ content. After recovery from the Exploratory Studies Facility (ESF), the cores may dry out at the Sample Management Facility at the Nevada Test Site. They are then machined into specimens using water as a coolant, and they dry out again in the laboratory until testing. During thermal conductivity and thermal expansion tests, specimens dry out in response to the elevated temperatures. Previous work (Brodsky et al. 1997, Brodsky 1997c) has shown that for welded tuff moisture content has no appreciable effect on thermal expansion; however, added moisture increases thermal conductivity values. For all specimens but one, there was a net decrease in thermal conductivity during testing that may be related to specimen drying. Moisture contents for mechanical specimens were measured after testing was completed.

3 TEST METHODS

3.1 Thermal conductivity

Thermal conductivity measurements were made using the guarded heat flow meter (GHFM). The test specimen was located between two heater plates controlled at different temperatures, producing heat flow through the specimen. The heat flow was measured by a heat flux transducer (HFT) located between the specimen and one heater plate. Radial heat flow losses were minimized in two ways: (1) A cylindrical guard heater surrounded the specimen and was maintained near the mean specimen temperature. (2) Specimens with lengths less than 20 mm were used.

The GHFM is calibrated by comparing theoretical values to results obtained using specimens of known thermal conductivity. A single set of calibrations is performed to determine both the contact resistance between the specimen and heater plates and the proportionality constant relating the output of the heat flux transducer to the actual heat flux. Calibrations were performed on reference samples of Pyrex 7740. A range of thermal resistance values was obtained using specimens of different thicknesses (6, 9, 12, 15, and 18 mm). Thermal resistance measurements were made at five temperatures (30°, 70°, 110°, 150°, and 200°C) spanning the operating range. Calibrations were verified by performing measurements on reference specimens of high-purity (99.99%) fused quartz using three specimen sizes spanning the operating range and testing at each of the five temperatures. Verifications were performed periodically (at least every 31 days) throughout the testing program. Pre-test verification errors were below 0.1 W / (mK). This is an indication of the difference in results obtained on the two types of reference materials. The National Institute of Standards and Technology (NIST)-recommended values for each standard are accurate only to $\pm 5\%$, so a disparity of 0.125 W / (mK) is within the error range to be expected. The difference between pre-test and subsequent verifications is an indication of apparatus reproducibility and drift over time at a specific thermal resistance. Apparatus output was reproducible and drift was not significant [< 0.04 W / (mK)].

After the instrument was calibrated, the test specimens were tested in the same manner as the reference materials. Specimens were placed in the apparatus and temperature was increased at 1°C/min. to each measurement temperature. Data were obtained after the instrument had reached steady-state thermal equilibrium as determined by taking readings of the thermocouples and HFT as a function of time until the readings were constant.

3.2 Thermal expansion

All the thermal expansion data were obtained from experiments using one of two identical push-rod dilatometer instruments manufactured by Harrop Industries. The specimen is placed in a receptacle at the end of a tube made of fused silica. The tube, or specimen holder, containing the specimen and push rod slides into a cylindrical furnace so that the specimen is positioned near the center of the furnace. As the temperature of the specimen changes, its length changes; this motion is transmitted to the push rod. The change in length is continuously measured by a linear variable displacement transformer (LVDT) located outside the heated area. A Type-K thermocouple near the surface of the specimen measures specimen temperature.

The test specimen was placed in the notched end of a fused silica tube and the test apparatus was set up as described. The furnace temperature was ramped up and down at a constant rate of 1°C/min. Displacement and temperature data were acquired continuously throughout the heating and cooling phases of the test and recorded by a computerized data acquisition system (DAS). The mean coefficient of thermal expansion ($\bar{\alpha}$ or MCTE) is the linear thermal expansion per unit change in temperature. It was calculated in approximately 25°C intervals. The strain-versus-temperature data were fit over each temperature interval using a linear least squares regression, and the slope of the linear fit provided values of α .

The dilatometer system expansion was calibrated and then verified by running Standard Reference Materials (SRMs) traceable to NIST and comparing data with expected results. Verifications were performed periodically (at least every 31 days) throughout the testing program and were considered acceptable only if the errors were less than 1 microstrain/°C.

3.3 Mechanical properties

Mechanical test specimens were used in unconfined compression tests. Specimens were monotonically loaded to failure while axial force, and axial and lateral deformations were monitored. These measurements were used to determine ultimate strength, Young's modulus, and Poisson's ratio.

Specimens were placed in flexible jackets to maintain constant moisture content during testing and contain the specimen fragments during failure. Ports were cut out of each jacket at the requisite locations to accommodate axial and lateral deformation gages. The axial displacement gage consisted of two LVDTs, located on opposite sides of the specimen. The LVDT barrels were located in a ring which was attached approximately one specimen radius above the specimen mid-height. The cores were on extended rods that rested in cups located on a lower ring placed approximately one specimen radius below specimen mid-height. The axial displacement gage therefore measured displacements occurring over the central section of the specimen. Radial strains were measured across one diameter of the specimen at mid-height using the radial displacement gage developed by Holcomb & McNamee (1984). This gage consisted of an LVDT mounted in a ring which is spring-loaded against the specimen. The barrel of the LVDT was mounted in the ring, and the core of the LVDT was attached to a leaf spring that directly contacted the specimen surface. Changes in specimen diameter directly displaced the LVDT core relative to the barrel. The accuracies of calibrations for both the axial and lateral displacement gages were within $\pm 2\%$ of reading over the verified range of 10–100% of full scale.

Tests were conducted in a servo-controlled hydraulic loading frame. The servo-controller was operated in strain-control feedback mode and force was applied such that a constant axial strain rate of 10^{-5} s⁻¹ was imposed. Specimens were unloaded after passing the peak in axial force. Strains were calculated by dividing the measured axial and lateral displacements by the current gage separations. The axial gage consisted of two LVDTs and the average axial strain is reported. Peak stress is the peak force divided by the current cross-sectional area of the specimen. The static elastic constants were calculated by performing linear least squares fits to the data collected between 10% and 50% of the stress difference at failure. Young's modulus is the slope of the linear fit to the axial strain versus axial stress data, and Poisson's ratio is the slope of the linear fit to the axial strain versus lateral strain data.

Before testing, after testing, and periodically during testing, validation tests were performed on 6061 aluminum to validate the test method. For the pre-test validation, measurements of Young's modulus and Poisson's ratio differed from the expected values by 3.4% and 4.8%, respectively. Measurements of Young's modulus and Poisson's ratio differed from the expected values by -1.5% and -2.6%, respectively, for the mid-test validation, and by 1.2% and 0.0%, respectively, for the post-test validations.

4 RESULTS

4.1 Thermal conductivity

The thermal conductivity data are summarized in Table 1 for post-test characterization. Data are grouped according to orientation and location with respect to the approximate maximum extent of the 100°C isotherm. Mean values of thermal conductivities ranged from 1.6 to 1.8 W / (mK) with an average thermal conductivity of 1.7 ± 0.1 W / (mK).

Figure 2 shows thermal conductivities measured during heating in this study and also for the pre-test characterization data (Brodsky 1996). The post-test data generally fall within the scatter of the pre-test results. The large scatter in the pre-test data, which should be noted, may indicate that there was some problem with this data set. The overlap of pre-test and post-test values would indicate that conducting the SHT did not affect conductivities; however, there appear to be differences between post-test specimens that were inside and outside of the approximate maximum extent of the 100°C isotherm. Figure 3 shows the post-test conductivities grouped by specimen orientation and location with respect to the approximate maximum extent of the 100°C isotherm. The data for a given temperature are plotted slightly offset from one another on the temperature

Table 1. Thermal conductivities for SHT post-test specimens.

Sample ID	Thermal Conductivity [(W / (mK))]									
	30°C	70°C	Heating	110°C	150°C	200°C	150°C	110°C	70°C	30°C
Outside 100°C Isotherm, Perpendicular to Heater										
N =	4	4		4	4	4	4	4	4	4
Mean =	1.74	1.73		1.72	1.71	1.69	1.65	1.64	1.65	1.69
STD =	0.08	0.06		0.06	0.06	0.06	0.06	0.06	0.07	0.07
Outside 100°C Isotherm, Parallel to Heater										
N =	4	4		4	4	4	4	4	4	4
Mean =	1.72	1.72		1.71	1.67	1.65	1.61	1.60	1.61	1.65
STD =	0.11	0.11		0.10	0.10	0.09	0.09	0.10	0.10	0.11
Inside 100°C Isotherm, Perpendicular to Heater										
N =	1	1		1	1	1	1	1	1	1
Mean =	1.83	1.82		1.83	1.81	1.79	1.77	1.75	1.76	1.82
Inside 100°C Isotherm, Parallel to Heater										
N =	7	7		7	7	7	6	6	6	6
Mean =	1.81	1.80		1.77	1.75	1.73	1.70	1.69	1.70	1.75
STD =	0.05	0.04		0.04	0.04	0.04	0.04	0.04	0.05	0.05
All Data										
N =	16	16		16	16	16	15	15	15	15
Mean =	1.77	1.77		1.75	1.72	1.71	1.67	1.66	1.67	1.71
STD =	0.08	0.08		0.07	0.07	0.07	0.07	0.07	0.08	0.08
All Data, All Temperatures										
N = 140	Mean = 1.71			STD = 0.08						

N = Number of Samples; STD = Standard Deviation.

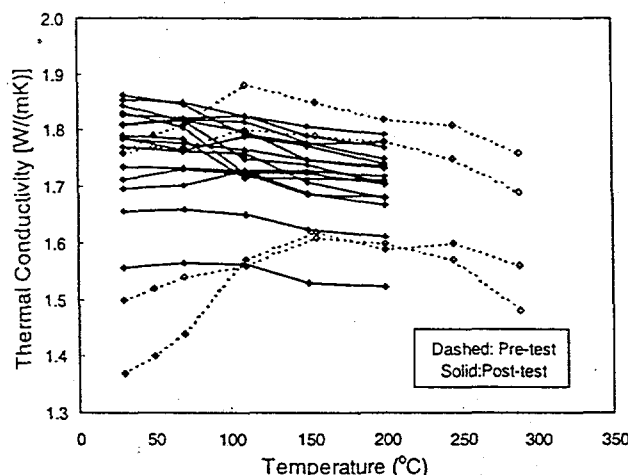


Figure 2. Thermal conductivities measured during heating for pre- and post-test SHT characterizations.

axis so that the error bars can be viewed easily. Although the error bars overlap (error bars represent \pm one standard deviation), the specimens from outside the isotherm generally have lower conductivities than those from within the isotherm. For reference, the thermal conductivities measured during characterization of Alcove 5 are also shown. These specimens were oven-dried before testing and so the conductivity values are expected to be below those measured in this study. At the higher test temperatures, after the post-test specimens have dried some-

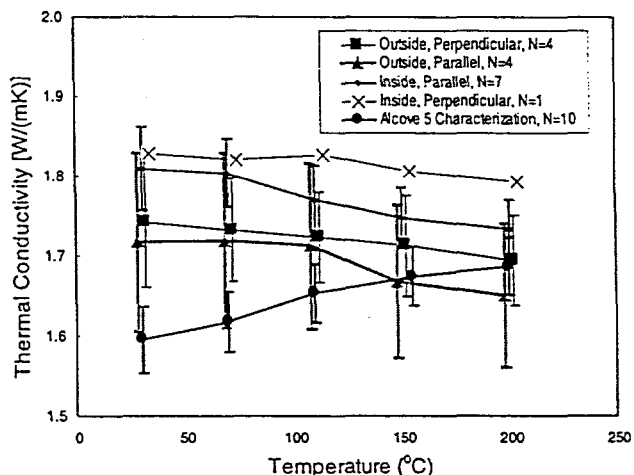


Figure 3. Thermal conductivities measured during heating for post-test SHT specimens categorized by orientation and location relative to approximate maximum extent of the 100°C isotherm (additional relevant Alcove 5 data shown for comparison).

what in the thermal conductivity apparatus, the Alcove 5 characterization values and values for post-test specimens from outside the 100°C isotherm overlap. The differences between specimens that appear to be related to their location relative to the 100°C isotherm are maintained during cooling (Finley et al. 1998).

4.2 Coefficient of thermal expansion

The mean coefficients of thermal expansion (MCTEs) are summarized in Table 2 for heating during the first thermal cycle. Data are categorized as being either from within or outside the approximate maximum extent of the 100°C isotherm, and either perpendicular or parallel to the heater. The MCTEs and standard deviations about each mean are given at each temperature for each category.

Figure 4 is a summary of MCTE versus temperature data obtained from different parts of Alcove 5. The data for a given temperature interval are plotted slightly offset from one another on the temperature axis so that the error bars can be viewed easily. The SHT post-test data from parallel and perpendicular specimens have been combined because there were no notable differences. All data sets show steep increases in MCTE beginning at approximately 150–200°C and continuing until approximately 300°C, with the steepest increases between 250° and 300°C. This steep increase is attributed to phase changes in the silica mineral phases. The MCTEs calculated over the temperature interval of 300–325°C decrease

as the phase change is completed. Specimens from outside the 100°C isotherm have similar values to those from other parts of Alcove 5, and plot above MCTEs from inside the 100°C isotherm. The SHT pre-test characterization data are closely matched to the post-test data from within the 100°C isotherm.

4.3 Elastic moduli and unconfined compressive strengths

Fourteen post-test specimens were tested in unconfined compression; the experimental data are summarized in Table 3. Young's moduli and peak stress values are lower outside the isotherm than inside the isotherm. Poisson's ratios also appear to differ; however, if one outlier (with a Poisson's ratio of 0.39) were to be omitted, then the Poisson's ratios would be almost the same for the two groups of data. Table 3 also compares elastic moduli and peak stress values obtained during the pre-test and post-test characterizations. Mean values of Young's modulus and peak stress are both lower for the post-test characterization data; however, the differences between the mean values are well within one standard deviation.

Table 2. MCTEs during first cycle heating of post-test SHT characterization specimens.

	MCTE During Heating ($10^{-6}/^{\circ}\text{C}$)												
	25- 50	50- 75	75- 100	100- 125	125- 150	150- 175	175- 200	200- 225	225- 250	250- 275	275- 300	300- 325	
Perpendicular to Heater, Outside 100°C Isotherm													
N =	3	3	3	3	3	3	3	3	3	3	3	3	3
Mean =	9.0	10.4	9.8	10.7	11.6	12.6	13.2	17.2	25.6	44.2	66.2	49.2	
STD =	0.3	0.7	0.1	0.5	0.7	0.4	1.2	1.9	6.4	11.6	7.7	3.4	
Perpendicular to Heater, Inside 100°C Isotherm													
N =	1	1	1	1	1	1	1	1	1	1	1	1	1
Mean =	9.0	10.1	8.9	9.4	10.8	12.9	13.5	16.0	20.4	30.6	51.4	54.0	
Parallel to Heater, Outside 100°C Isotherm													
N =	4	4	4	4	4	4	4	4	4	4	4	4	4
Mean =	8.8	10.2	8.6	9.5	10.4	11.5	11.7	14.9	23.4	33.5	61.5	57.5	
STD =	0.1	0.3	0.3	0.1	0.2	0.3	0.7	1.5	7.3	4.9	14.3	10.6	
Parallel to Heater, Inside 100°C Isotherm													
N =	6	6	6	6	6	6	6	6	6	6	6	6	6
Mean =	8.2	9.4	8.8	9.3	10.3	11.3	12.2	14.7	19.3	28.8	50.5	56.1	
STD =	0.5	0.6	0.4	0.3	0.3	0.5	0.6	1.2	3.2	5.1	10.3	9.4	
All Data Outside 100°C Isotherm													
N =	7	7	7	7	7	7	7	7	7	7	7	7	7
Mean =	8.9	10.3	9.1	10.0	10.9	12.0	12.3	15.9	24.4	38.1	63.5	54.0	
STD =	0.2	0.4	0.7	0.7	0.8	0.7	1.2	2.0	6.5	9.5	11.3	8.9	
All Data Inside 100°C Isotherm													
N =	7	7	7	7	7	7	7	7	7	7	7	7	7
Mean =	8.3	9.5	8.8	9.3	10.4	11.5	12.3	14.9	19.4	29.1	50.6	55.8	
STD =	0.5	0.6	0.4	0.2	0.3	0.8	0.8	1.2	3.0	4.7	9.4	8.6	
All Data													
N =	14	14	14	14	14	14	14	14	14	14	14	14	14
Mean =	8.6	9.9	9.0	9.6	10.6	11.8	12.3	15.4	21.9	33.6	57.1	54.9	
STD =	0.5	0.7	0.6	0.6	0.6	0.7	1.0	1.7	5.5	8.6	12.0	8.5	

N = Number of Samples; STD = Standard Deviation

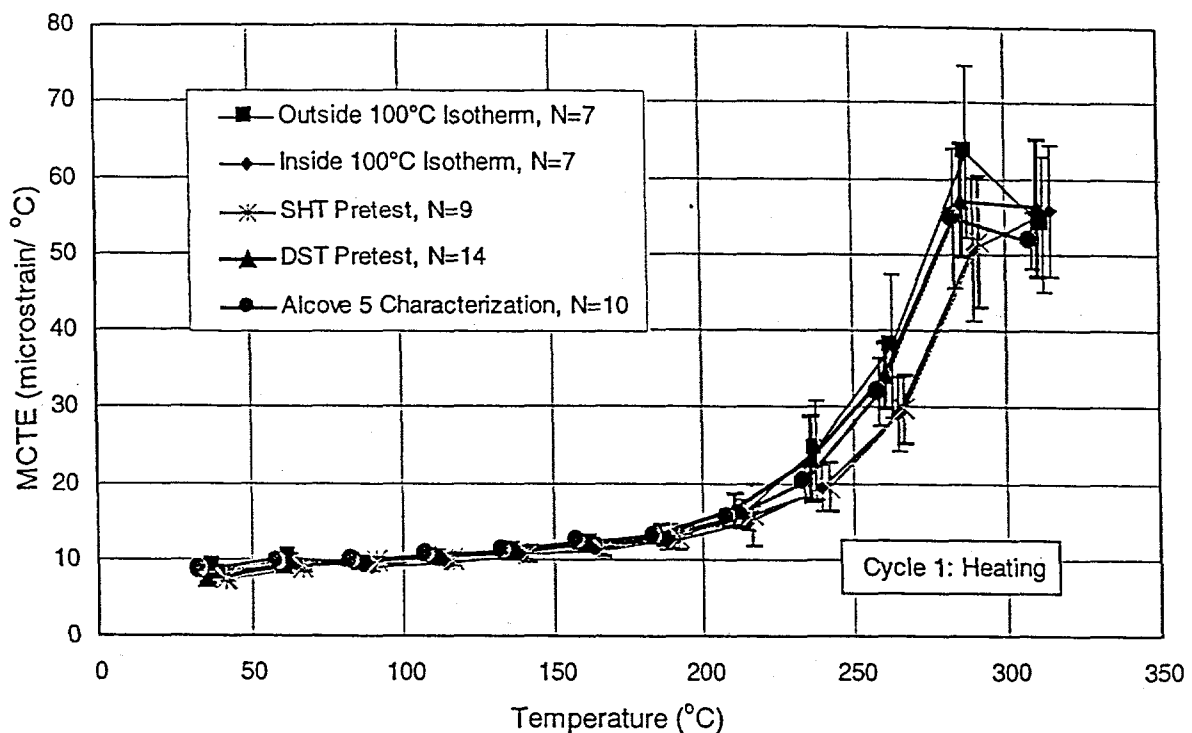


Figure 4. Mean coefficients of thermal expansion-versus-temperature during first heating for all Alcove 5 data sets. The legend provides the number of specimens tested. Error bars represent \pm one standard deviation.

Table 3. Comparison of mechanical data from Single Heater and Drift Scale test areas, and from surface drillholes.

Test Region	Young's Modulus (GPa)			Poisson's Ratio			Unconfined Compressive Strength (MPa)		
	Mean	Standard Devia-tion	No. of Tests	Mean	Standard Devia-tion	No. of Tests	Mean	Standard Devia-tion	No. of Tests
SHT Post-test: Inside 100°C Isotherm	33.3	3.6	9	0.18	0.04	9	151.1	68.7	9
SHT Post-test: Outside 100°C Isotherm	28.4	5.4	5	0.23	0.09	5	103.1	68.7	5
SHT Post-test: All	31.6	4.8	14	0.20	0.07	14	134.0	70.2	14
SHT Pre-test	32.4	2.9	22	0.17	0.02	22	143.2	50.3	22
DST Pre-test	36.8	3.5	16	0.20	0.04	16	176.4	65.8	16
NRG-5 drillhole	32.5	10.8	8	0.20	0.06	8	173.3	99.4	8
NRG-6 drillhole	32.1	3.0	8	0.19	0.03	8	193.0	55.7	8
NRG-7/7A drillhole	33.2	4.2	19	0.22	0.03	19	192.1	51.1	9
SD-9 drillhole	32.8	5.1	15	0.21	0.02	15	189.1	64.8	7
SD-12 drillhole	34.3	2.0	4	0.20	0.01	4	195.8	3.5	2
Difference: SHT Pre-test vs. all SHT Post-test	-2.5%			16%			-6.6%		

Mean Poisson's ratio is higher for the post-test characterization. In this case, the difference between mean values is greater than the standard deviation obtained for the pre-test suite but within one standard deviation of the post-test values. The post-test mean Poisson's ratio is heavily influenced by one outlier with a ratio of 0.39.

Elastic moduli and peak stresses for the SHT can be compared with data from the DST pre-test char-

acterization (Brodsky 1997a) and from borehole characterizations (US DOE 1996) given in Table 3. There were minor differences in the testing programs that should not have had any significant effects on the results.

The data distributions for Young's modulus and peak stress are given in Figures 5 and 6, respectively. Each figure shows data from the pre-test and post-test SHT characterizations. Figure 5 shows that the

Young's moduli are evenly distributed about the mean (32.4 GPa) for the pre-test specimens. However only four post-test specimens have Young's moduli below the post-test mean (31.6 GPa), whereas ten post-test specimens have values above the mean. The pre-test and post-test peak strength values are both approximately evenly distributed about their respective means.

5 DISCUSSION OF RESULTS

The SHT post-test thermal and mechanical properties data were compared with pre-test SHT data in the previous section. The comparisons are summarized as follows:

- Thermal conductivities fell within the range defined by the pre-test measurements. Conductivities for specimens outside the approximate maximum extent of the 100°C isotherm were below those of specimens from inside the isotherm.
- Thermal expansion coefficients for post-test specimens from within the approximate maximum extent of the 100°C isotherm were below those of specimens from outside the isotherm. Values for pre-test specimens were approximately coincident with those for post-test specimens from within the 100°C isotherm.
- Unconfined compression tests provided a mean peak stress value that was 9 MPa below the pre-test values. The standard deviations for mean peak stresses were 50–70 MPa and so this decrease is not significant. Young's moduli and peak stresses were lower for specimens outside the approximate maximum extent of the 100°C isotherm than inside the isotherm.
- No anisotropy was evident, consistent with conclusions reported in Brodsky (1997c).

A consistent explanation for the differences between pre-test and post-test results and the differences between values inside and outside the approximate maximum extent of the 100°C isotherm was not found. It was expected that within the 100°C isotherm, cracking might occur from higher thermal gradients, differential thermal expansion of minerals, or steam pressure resulting from the vaporization of non surface-connected water. Greater damage would be indicated by lower strengths, lower measured values of Young's moduli, lower thermal conductivities, and lower thermal expansion coefficients. (Thermal expansion coefficients would be lowered if thermal expansion during laboratory tests were taken up by volume expansion into newly formed cracks.)

The data do not show consistent evidence that damage was greater inside the approximate maximum extent of the 100°C isotherm. Specimens from

inside the isotherm exhibited lower thermal expansion coefficients than those from outside of the isotherm, consistent with the hypothesis that specimens from inside the 100°C isotherm were more damaged than those from outside the isotherm. In addition, coefficients of thermal expansion from other locations in Alcove 5 most closely matched results obtained outside the isotherm. However, additional data do not indicate greater damage within the 100°C isotherm. The thermal expansion data from inside the isotherm closely matched the pre-test thermal expansion values. Also, lower Young's moduli, strengths, and thermal conductivities were obtained outside the maximum extent of the 100°C isotherm than inside. These data indicate that for the intact sections of rock tested here, rocks inside the isotherm were not more damaged than those outside.

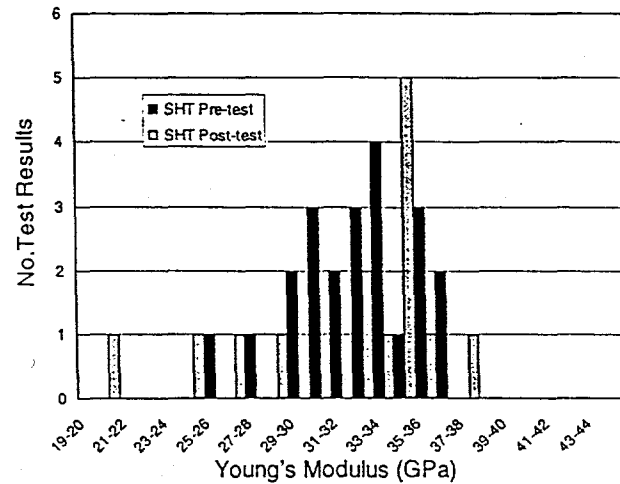


Figure 5. Distribution of Young's modulus values obtained for pre-test and post-test specimens from the SHT block.

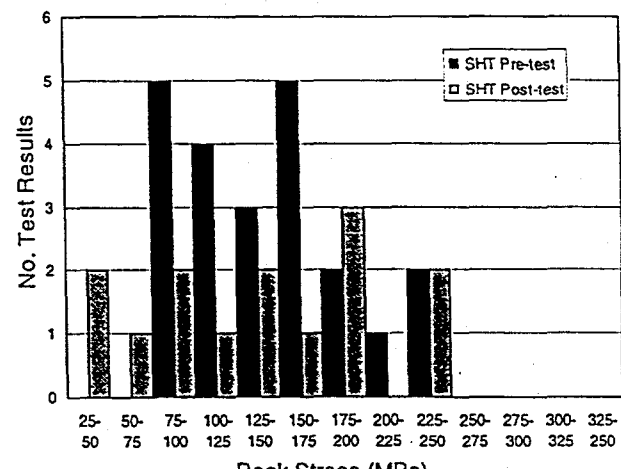


Figure 6. Distribution of peak stress values obtained for pre-test and post-test specimens from the SHT block.

The role of moisture content was also evaluated. It might be expected that specimens from inside the 100°C isotherm would be drier than those from outside. All specimens were cored and ground under water and then allowed to dry in the laboratory at room temperature until testing. The specimens were then tested "as is." If the specimens from inside the 100°C isotherm remained drier than those from outside, it would be expected that those from inside the isotherm would have higher strengths and lower thermal conductivities. Thermal expansion and elastic moduli should be relatively unaffected by moisture content. The data did show that strengths were higher for specimens from inside the isotherm, consistent with the idea that these specimens were drier; however, thermal conductivities showed the opposite. Conductivities from inside the isotherm were higher than those from outside, indicating that specimens from the interior were not drier than those from outside the isotherm. These data indicate that differences in moisture content that may have existed in situ were not sufficiently preserved to affect the laboratory properties data.

6 CONCLUSIONS

The objectives of this study were to characterize the post-test SHT area and to evaluate changes in rock properties that might have resulted from conducting the SHT. Thermal conductivity values fell within the range defined by pre-test characterization activities. Specimens from outside the approximate maximum extent of the 100°C isotherm generally had lower thermal conductivities than those from the interior. Thermal expansion coefficients for specimens from within the 100°C isotherm were well matched to those obtained during pre-test characterization tests. Those from outside the isotherm were higher and more closely matched to existing data collected on specimens from other parts of Alcove 5. Unconfined compressive strengths and Young's moduli were slightly, but not significantly, reduced as compared to pre-test values. Strengths and Young's moduli from inside the 100°C isotherm were higher than values obtained outside the isotherm.

The data were evaluated and found to be not completely consistent with the hypothesis that there was increased damage within the approximate maximum extent of the 100°C isotherm. Similarly, the data showed no indication that differences in moisture content were retained through the specimen preparation process. No consistent explanation for the differences between pre-test and post-test results and the differences between values inside and outside of the 100°C isotherm was found. The major

conclusion for repository design and performance assessment is that the thermal cycle imposed by the SHT had no significant impact on long-term thermal-mechanical intact rock properties.

REFERENCES

Boyd, P.J., J.S. Noel, T.N. Hill, & R.J. Martin III 1996. TDIF 305602. Unconfined compression tests on specimens from the Single Heater Test area in the Thermal Testing Facility at Yucca Mountain, Nevada. Data Tracking Number: SNL22080196001.002.

Brodsky, N.S. 1996. TDIF 305593. Thermal properties of test specimens from the Single Heater Test area in the Thermal Testing Facility at Yucca Mountain, Nevada. Data Tracking Number: SNL22080196001.001.

Brodsky, N.S., M. Riggins, J. Connolly, & P. Ricci 1997. *Thermal expansion, thermal conductivity, and heat capacity measurements for boreholes UE25 NRG-4, UE25 NRG-5, USW NRG-6, and USW NRG-7/7A.* SAND95-1955. Albuquerque, NM: Sandia National Laboratories.

Brodsky, N.S. 1997a. TDIF 306126. Unconfined compression tests on specimens from the Drift Scale Test area of the Exploratory Studies Facility at Yucca Mountain, Nevada. Data Tracking Number: SNL22100196001.001.

Brodsky, N.S. 1997b. TDIF 306127. Thermal expansion and thermal conductivity of test specimens from the Drift Scale Test area of the Exploratory Studies Facility at Yucca Mountain, Nevada." Data Tracking Number: SNL22100196001.001.

Brodsky, N.S. 1997c. TDIF 306294. Laboratory measurements of thermal expansion and thermal conductivity for specimens from Alcoves 5 and 7 of the Exploratory Studies Facility and from SD drillholes at Yucca Mountain, Nevada. Data Tracking Number: SNL22100196001.002.

Finley R.E., S. Ballard, N.S. Brodsky, N.D. Francis, J.T. George, & S.R. Sobolik 1998. TDIF 307112. Single Heater Test final report. Data Tracking Number: SNF35110695001.009.

Holcomb, D.J. & M.J. McNamee 1984. *Displacement gage for the Rock Mechanics Laboratory.* SAND84-0651. Albuquerque, NM: Sandia National Laboratories.

US DOE (US Department of Energy). 1996. Civilian radioactive waste management system management and operating contractor. Yucca Mountain Site Geotechnical Report BAAA00000-01717-4600-00065 REV 00. Las Vegas, NV: US DOE.